Theor Chem Acc (1997) 96:261–268

Theoretical
Chemistry Accounts

Assignment of conformation-sensitive near-infrared bands in high-spin ferrous haemoproteins.

Low-temperature magnetic circular dichroism data

Vasily S. Oganesyan, Yuri A. Sharonov

The Engelhardt Institute of Molecular Biology, Academy of Sciences of Russia, 117984 Moscow, Russia

Received: 4 February 1997 / Accepted: 1 May 1997

Abstract. An assignment of the near-infrared bands in the 600–800 nm spectral region observed in magnetic circular dichroism (MCD) spectra of high-spin ferrous haemoproteins is presented. The assignment is based on a relative energy level scheme for iron *d*-electrons, a comparison of predicted and measured temperature dependences of MCD intensity, a sign of MCD bands and a group theoretical analysis of allowed transitions. The proposed assignment is consistent with the ~15-nm red shift of the ~760 nm band on breakage of the Fe-His bond in deoxy-myoglobin at low pH, with low-temperature photolysis experiments available for CO complexes of several haemoproteins. In accordance with the observations, the intensity of the MCD bands for proteins with a sulphur anion of cysteine as proximal haemligand (cytochrome P450 and chloroperoxidase) is predicted to be diminished by at least one order of magnitude compared to that for proteins with an imidazole of a histidine as a protein-derived haemligand (i.e. myoglobin, haemoglobin and horseradish peroxidase).

Key words: Magnetic circular dichroism – Haemoproteins – Haem electronic structure – Near-infrared band assignment

1 Introduction

Haem proteins and enzymes constitute an important class of biomolecules that mediate a wide variety of biological functions. They all have a haem group in the active site. Since the electronic structure of the haem plays a central role in the biochemical activity of haemoproteins, its investigation is very important for understanding the functional diversity of these proteins. Spectroscopic methods have proved to be useful tools for such studies.

* *Correspondence to*: Y.A. Sharonov (shar@genom-ii.eimb.rssi.ru)

Myoglobin (Mb), haemoglobin (Hb), leghaemoglobin and horseradish peroxidase (HRP) in the high-spin ferrous state have weak transitions in the near-infrared region of 600–1000 nm which have been revealed by optical absorption [1–4], magnetic circular dichroism (MCD) [2, 5–9] and natural circular dichroism (CD) [2] spectroscopy. Iizuka et al. [1] have studied the properties of a well-resolved absorption band at ~760 nm (band III, [2]) in products obtained by photodissociating the CO complexes of Mb and Hb at 4.2 Kelvin (K). For both proteins they observed about a 10-nm red shift of band III in the photoproducts as compared to the deoxy-preparations under the same conditions. Other groups have confirmed these findings with photolysis at low [10–17] or room temperature [18] using time-resolved absorption spectroscopy. Near-infrared absorption has been used to follow oxygenation levels of Hb and Mb in human smooth and striated muscle [18] or in cardiac muscle [19] in vivo.

Because of the sensitivity of band III to the local conformation near the haem iron, Iizuka et al. called it the "conformation band" [1]. In addition to the positive band at ~760 nm, there are two other well-resolved bands in MCD spectra of unligated ferrous haemoproteins which are obscured in the absorption spectra. These are the positive band at ~680 nm (band IV, [2]) and the negative band at ~630 nm (band V) [6–9]. The positions of bands III, IV and V in the MCD spectra of various unligated ferrous haemoproteins and of a five-coordinate protohaem-(2-methylimidazole) complex have been compared with those of the metastable photoproducts of their O_2 and/or CO adducts generated at 4.2 K [6, 8, 9]. The results were interpreted in terms of restrictions imposed by the protein moiety to the geometrical alteration of Fe-porphyrin and Fe-His bonds on ligand binding or release. A correct spectroscopic assignment of the near-infrared bands is important to allow a more fundamental interpretation of studies, based on observation of these bands, in terms of structural changes in the active site followed by ligand and/or substrate binding as well as conformational changes of the protein moiety.

Several attempts have been made to classify transitions in the near-infrared spectral region. On the basis of polarized single-crystal absorption, solution natural CD and room temperature MCD spectra as well as extended Hückel calculations, Eaton et al. [2] have assigned band III to a $\overline{a}_{2u}(\pi) \rightarrow \overline{d}_{yz}$ charge transfer (CT) transition. Alternatively, on the basis of self-consistent field, (SCF-LCAO-ASMO) and configuration interaction (CI) calculations of low-lying multiplets and optically allowed exited states and a computation of the near-infrared *xy*-polarized MCD bands for a high-spin ferrous haem with bound imidazole, Seno et al. [19, 20] assigned band III to a $\overline{d}_{xz} \rightarrow \overline{d}_{z2}$ ligand field transition. Later, on the basis of a single-crystal absorption spectra and iterative extended Hückel (IEH) calculations, band III in deoxy-Mb was assigned by Makinen and Churg [21] as a $d_{x2-y2} \rightarrow e_g(\pi^*)$ CT transition. This assignment contradicts the single crystal results of Eaton et al. [2], which indicate either an *x*- or *y*-polarized band instead of an *xy*-polarized one. Moreover, Sage et al. [22] refused such an assignment because they observed band III for a four-coordinate ferrous haem in deoxy-Mb at low pH. Such a haem with the $S = 1$ ground state has a vacant d_{x2-y2} orbital [23, 24]. Band IV in deoxy-Hb was attributed to a $\overline{a}_{1u}(\pi) \rightarrow \overline{d}_{yz}$ CT transition and to a vibronic satellite of a $d_{x2-y2} \rightarrow e_g(\pi^*)$ CT transition by Eaton and co-workers [2] and by Makinen and Churg [21], respectively.

At last, band V was assigned either to a $d_{z2} \rightarrow e_g(\pi^*)$ CT transition [21] or mainly to a $\overline{d}_{xz} \rightarrow \overline{b}_{2u}(\pi^*)$ CT transition [19, 20]. Thus, the existing experimental data and theoretical considerations do not provide unambiguous classification of orbital promotions responsible for the near-infrared transitions in the $S = 2$ ground state of the ferrous haem. Moreover, not all possible promotions which could be responsible for observed bands have been considered. Additional observations and theoretical analysis are desirable for more strict assignment. The results of temperature-dependent MCD studies of high-spin Fe(II) haemoproteins may be of great importance, as emphasized by Eaton and co-workers [2].

In this paper be discuss the following. First, we present theoretical analysis showing that temperature-dependent MCD spectra provide new arguments for the assignment of the near-infrared bands in spectra of high-spin ferrous haemoproteins. Second, we show that our assignments are consistent with those given by Eaton et al. [2] for bands III and IV, and by Seno et al. [20] for band V. Third, we provide an interpretation to multi-band MCD observed between bands III and IV. Lastly, we provide evidence that the intensity of assigned MCD bands for reduced cytochrome P450 should be smaller, at least, by one order of magnitude than those for deoxy-Mb and reduced HRP. The intensity difference is associated with the various ground states, i.e. $^5E_\eta$ and $^5B_2$ in proteins with a histidine or cystainate as a protein-derived haem ligand, respectively [25]. It is important to note that the theoretical approach used in this paper can, in principle, be applied for analysis of *d*-*d* and CT transitions in MCD spectra of high-spin and low-spin ferric haemoproteins.

2 Theoretical background

From the calculations of the Coulomb repulsion within the $3d^6$ configuration in the tetragonal-point symmetry of the iron cation, Eicher and Trautwein [26] found that the states $^5B_2, ^5E, ^3E$ and $^1A_1$ have the lowest energy and are well separated from the next excited states. The multi-electron functions corresponding to these terms are represented by the Slater determinants: $^5B_2 \sim |\xi\eta\zeta u\ v\overline{\zeta}\ldots|$, $^5E_\eta \sim |\xi\eta\zeta uv\overline{\eta}\ldots|$, $^5E_\xi \sim |\xi\eta\zeta uv\overline{\xi}\ldots|$, $^3E_\eta \sim |\xi\eta\zeta u\overline{\eta}\overline{\zeta}\ldots|$, $^3E_\xi \sim |\xi\eta\zeta u\overline{\xi}\overline{\zeta}\ldots|$, $^1A_1 \sim |\xi\eta\overline{\zeta}\xi\eta\overline{\zeta}\ldots|$ in which η, ξ, ζ, u, v are molecular orbitals composed mainly of $3d$ atomic orbitals, $\eta \approx d_{xz}$, $\xi \approx d_{yz}$, $\zeta \approx d_{xy}$, $u \approx d_{z2}$, $v \approx d_{x2-y2}$, and the closed-shell part of ligand molecular orbitals is not written down explicity. The molecular *x*- and *y*-axes are defined through the pyrrole nitrogen atoms. The rhombic distortions split the $^5E(^3E)$ level into $^5E_\eta(^3E_\eta)$ and $^5E_\xi(^3E_\xi)$, and the spin-orbit and Zeeman interactions finally split all levels into 22 singlets.

In our previous paper [25] we carried out analysis of the electronic level scheme of the high-spin ferrous haem in Mb, HRP and cytochrome P450 by simultaneous fit of adjustable parameters of the four-term theoretical model to the variable-temperature MCD, room-temperature absorption in the Soret spectral region and available magnetic susceptibility and/or Mössbauer data. The evidence suggests that there are large distinctions between the shape, intensity and temperature behaviour of the Soret MCDs of Mb and HRP compared to those of cytochrome P450. These differences can be described only if the ground manifold in these proteins contains one component of the split term i.e., ^5E (Mb and HRP) and $^5B_2$ (P450).

After taking into account the spin-orbit and Zeeman interactions within the six low-lying states in the C_{2v} symmetry, the lowest five eigenfunctions are generally written as

$$|n\rangle = \sum_{\sigma=-S}^{S} \left\{ \sum_{S=1}^{2} \left(C_n, \hat{S}_{\eta\sigma} \left| {}^{2S+1}E_\eta, \sigma \right\rangle + C_{n,s\xi\sigma} \left| {}^{2S+1}E_\xi, \sigma \right\rangle \right) + C_{n,2\zeta\sigma} \left| {}^5B_2, \sigma \right\rangle \right\} + C_{n,A_1} \left| {}^1A_1 \right\rangle \ , \quad (1)$$

where σ denotes the quantum number of the *z*-component of the total spin S and the coefficients at base wavefunctions are the functions of magnetic field strength H. Once the parameters of the energy level scheme are determined for deoxy-Mb, reduced HRP and reduced cytochrome P450 [25] one can calculate the coefficients in the eigenvectors (Eq. 1) and energies of states. As shown below, knowledge of the eigenvectors and eigenvalues of the low-lying singlets allows calculation of the temperature dependence of MCD intensity which, together with the predicted sign of the MCD band for one-electron transition of a given symmetry, make it possible to assign the near-infrared transitions.

The sign of the MCD and its temperature behaviour can be predicted from modified general expressions given by Schatz et al. [27] for a molecule which has an

arbitrary orientation with respect to an external magnetic field:

$$\Delta\varepsilon(\vartheta,\varphi,H,T,v) = \frac{K}{Q_g}\sum_{n,j}\Lambda_{nj}\cdot\exp(-E_n/kT) \cdot f(v,v_{jn},\Delta_{jn}) \ , \quad (2)$$

where

$$\Lambda_{nj} = -2\ \mathrm{Im}\left\{\cos\vartheta\langle n|m_x|j\rangle\langle j|m_y|n\rangle + \sin\vartheta(\sin\varphi\langle n|m_x|j\rangle\langle j|m_z|n\rangle + \cos\varphi\langle n|m_y|j\rangle\langle j|m_z|n\rangle)\right\} \ ,$$

$$v_{jn} = (E_j - E_n)/h \quad \text{and} \quad Q_g = \sum_n \exp(-E_n/kT) \ .$$

Here $\Delta\varepsilon$ designates the difference between the molar extinction coefficients for left and right circularly polarized light, m_x, m_y, and m_z are the indicated components of the molecule-fixed transition dipole operator and θ, ϕ are two of three Eulerian angles describing the rotation of the molecular coordinate system with respect to the laboratory-fixed system whose z-axis is directed along the magnetic field H. K is a constant calculated to be 207.82 if the electric dipole moments are given in Debyes. Summations are over all regarded transitions $n \to j$. $f(v, v_{jn}, \Delta_{jn})$ is a band-shape function of the Gaussian type normalized in such a way that $\int(f(v,v_{jn})/v)\mathrm{d}v = 1$ and Δ_{jn} is a band width parameter.

As shown in [25], the perturbation theory for spin-orbit interaction is a good approximation independent of whether the haem ground state is ${}^5E_\eta$ (Mb and HRP) or ${}^5B_2$ (P450). In addition, since a band width is much larger than the energy spread between sublevels of any manifold, MCD for transitions from the ground manifold to an excited one can be approximated by one band. Since we deal with molecules in solution Eq. (2) must be averaged over all orientations. Taking this into account and substituting wavefunctions Eq. (1) into Eq. (2) for the case when ${}^5E_\eta$ is the ground state, we obtain for MCD effects of the first order

$$\left\langle \Delta\varepsilon\left({}^5E_\eta \to {}^5\Gamma\right)\right\rangle = K\cdot\sum_{\substack{i=z,x\\(j,k\neq i,\\ j\neq k)}} g_i(T,H)\cdot F_{jk}\cdot f(v,v_\Gamma,\Delta_\Gamma), \quad (3)$$

where Γ is one of the irreducible representation of the C_{4v}-point group.

The factors $g_z(T,H)$ and $g_x(T,H)$ are functions of both temperature and H and are determined as follows:

$$g_z(T,H) = \frac{1}{8\pi^2}\int_0^\pi\int_0^{2\pi}\int_0^{2\pi}\langle L_z\rangle\cdot\sin\vartheta\cdot\cos\vartheta\ \mathrm{d}\theta\ \mathrm{d}\varphi\ \mathrm{d}\psi$$

$$g_x(T,H) = \frac{1}{8\pi^2}\int_0^\pi\int_0^{2\pi}\int_0^{2\pi}\langle L_x\rangle\cdot\sin^2\vartheta\cdot\cos\varphi\ \mathrm{d}\theta\ \mathrm{d}\varphi\ \mathrm{d}\psi \quad (4)$$

where $\langle L_{z(x)}\rangle = \pm(2/Q_g)\cdot\sum_{n=1}^{5}\sum_{\sigma=-2}^{2}\mathrm{Im}\left\{C^*_{n,2\eta\sigma}\cdot C_{n,2\xi(\zeta)\ \sigma}\right\}\cdot\exp(-E_n/kT)$ $,\left(\left|C_{n,2\eta\sigma}\right|\approx 1, \left|C_{n,2\xi(\zeta)\sigma}\right|\approx 0.1\right)$.

Up to the first order, the net expectation value of the $z(x)$-component of an angular momentum is induced by magnetic field H and is always negative. The $g_i(T,H)$ factors are related to the average energy of interaction of an induced orbital angular momentum with a magnetic field through the formula:

$$\sum_{i=x,y,z} g_i(T,H) = \frac{\langle\beta\cdot\mathbf{H}\cdot\mathbf{L}\rangle}{\beta\cdot H} \ .$$

All integrals are evaluated numerically.

Table 1 displays the results of analysis of MCD features for transitions to excited states which transform as the functions of irreducible representations of the C_{4v}-point symmetry group (first column). The products of matrix elements $F_{jk} = \langle|m_j|\rangle\langle|m_k|\rangle$, which are nonzero by symmetry properties for a given Γ, are shown in the second and third columns of Table 1. The fourth column shows the polarization directions for a given transition; the predominant one is placed outside the brackets. For

Table 1. Analysis of the first-order effects of magnetic circular dichroism (MCD) for transitions to excited manifolds ${}^5\Gamma$ which belong to irreducible representations of the C_{4v}-point symmetry group

Γ[a]	F_{xy}	F_{yz}	Polarization	Sign	γ[b]		
					$\overline{\eta}\to\overline{\varphi}(\gamma)$	$\overline{\varphi}(\gamma)\to\overline{\xi}$	$\overline{\varphi}(\gamma)\to\overline{\zeta}$
A_1	$-\langle{}^5E_\eta\|m_x\|{}^5\Gamma\rangle\langle{}^5\Gamma\|m_y\|{}^5E_\xi\rangle$		$x(y)$[c]	+	a_1	a_2	
B_1	$-\langle{}^5E_\eta\|m_x\|{}^5\Gamma\rangle\langle{}^5\Gamma\|m_y\|{}^5E_\xi\rangle$		$x(y)$	−	b_1	b_2	
A_2	$+\langle{}^5E_\xi\|m_x\|{}^5\Gamma\rangle\langle{}^5\Gamma\|m_y\|{}^5E_\eta\rangle$		$y(x)$	+	a_2	a_1	
B_2	$+\langle{}^5E_\xi\|m_x\|{}^5\Gamma\rangle\langle{}^5\Gamma\|m_y\|{}^5E_\eta\rangle$	$-\langle{}^5E_\eta\|m_y\|{}^5\Gamma\rangle\langle{}^5\Gamma\|m_z\|{}^5B_2\rangle$	$y(x,z)$	Undefined	b_2		
	$+\langle{}^5E_\xi\|m_x\|{}^5\Gamma\rangle\langle{}^5\Gamma\|m_y\|{}^5E_\eta\rangle$		$y(x)$	−		b_1	
E_x		$-\langle{}^5B_2\|m_y\|{}^5\Gamma\rangle\langle{}^5\Gamma\|m_z\|{}^5E_\eta\rangle$	$z(y)$	Undefined	e_x		b_2

[a] Irreducible representation of the excited configuration
[b] The possible one-electron excitations allowed by the selection rules of electric dipole matrix elements correspond to an appropriate transition to a state ${}^5\Gamma\cdot\gamma$ is an irreducible representation of the molecular orbital φ^c
[c] Polarization directions for a given transition, the predominant one is given without brackets

transitions polarized in the haem plane, a sign of the product of matrix elements F_{xy} is determined by the properties of the symmetry transformation in the C_{4v}-point symmetry group [20]. Therefore, MCD bands for xy-polarized transitions have definite signs, which are shown in the fifth column. In the last three columns the one-electron promotions are indicated which satisfy selection rules for matrix elements of the electric dipole moments m_j and m_k.

Now we consider the case when the wavefunction of an excited state obtained after one-electron promotion belongs to a reducible representation. This situation is realized for an excitation from a degenerate orbital (but not the d_π-orbital) to a nondegenerate one or vice versa. The $\pi \rightarrow \pi^*$ transition in the Soret region is an example of such a promotion. Theoretical analysis of the Soret MCD is given in our previous publication [25]. It is shown that the $\pi - d$ configuration and spin-orbit interactions in the excited states together with a rhombic distortion at the haem, give rise to four overlapping MCD bands of opposite sign whose overall integrated intensity is zero. The four overlapping MCD bands of x, y polarization should also be observed for a CT transition of the $a_1, a_2, b_1, b_2 \rightarrow e$ type. However, because there is borrowing of intensity from other states of the same symmetry, the sign of each of the four MCD bands for weak CT transitions is undefined.

In conclusion two comments should be make. First, for the one-electron transitions considered above, Eqs. (3) and (4) derived for the $^5E_\eta$ ground state also remain correct for the $^5B_2$ ground state.

However, in the latter the $g_z(T,H)$ factor will be smaller at least by one order of magnitude than in the former, since both $C_{n,2\eta\sigma}$ and $C_{n,2\xi\sigma}$ coefficients are of first-order magnitude. Second, the sign analysis of the MCD bands given for the C_{4v}-point group is also applicable for C_{2v} symmetry since the porphyrin, as well as, the iron orbitals are assumed to be essentially unchanged under weak rhombic distortion.

3 Results and discussion

The near-infrared MCD spectra of deoxy-Mb and reduced HRP recorded at temperatures from 290 K to down 4.2 K [25] are shown in Fig. 1a and b, respectively. A contribution from the visible MCD has been subtracted from the spectra. Magnetic dichrographs and details of low-temperature measurements are described in [28]. We follow the numbering of the near-infrared bands given by Eaton et al. [2] in their studies of deoxy-Hb by room temperature MCD, natural CD and polarized single-crystal absorption spectroscopy. They labelled Gaussian components resolved by a fit procedure at $\sim$11000 cm^{-1}(910 nm), $\sim$12400 cm^{-1}(810 nm), $\sim$13200 cm^{-1}(760 nm) and $\sim$14800 cm^{-1}(675 nm) as bands I, II, III and IV, respectively. The positive MCD bands III and IV are clearly seen in the MCD spectra of Mb and HRP. The MCD spectra of both Mb and HRP also display negative bands at $\sim$15800 cm^{-1} (635 nm). We will refer to the bands in this region as bands V and Va. Figure 1a and b show the existence of several overlapping bands in the spectral region between bands III and IV. In the MCD spectrum of HRP all these bands are positive while there are positive and negative bands in this region of the MCD spectrum of Mb.

Our assignment is based on the results of the theoretical analysis given above as well as on the ligand field parameters and the energy level scheme for iron d-orbitals (Fig. 2) derived earlier for deoxy-Mb and reduced HRP from a fit of available experimental data to a four-term theoretical model [25]. We consider transitions mainly between d-orbitals $\eta(e_x) \approx d_{xz}, \xi(e_y) \approx d_{yz}, \zeta(b_2) \approx d_{xy}, u(a_1) \approx d_{z2}, v(b_1) \approx d_{x2-y2}$ and CT transitions involving these orbitals and the highest filled $a_{2u}(a_1)$, $a_{1u}(a_2)$ and the lowest empty $e_g(e), b_{1u}(b_2)$, $b_{2u}(b_1)$ prophyrin π-orbitals [2, 19, 29]. The porphyrin orbitals are labelled according to commonly used D_{4h} symmetry (labels shown in brackets are those of C_{4v} symmetry).

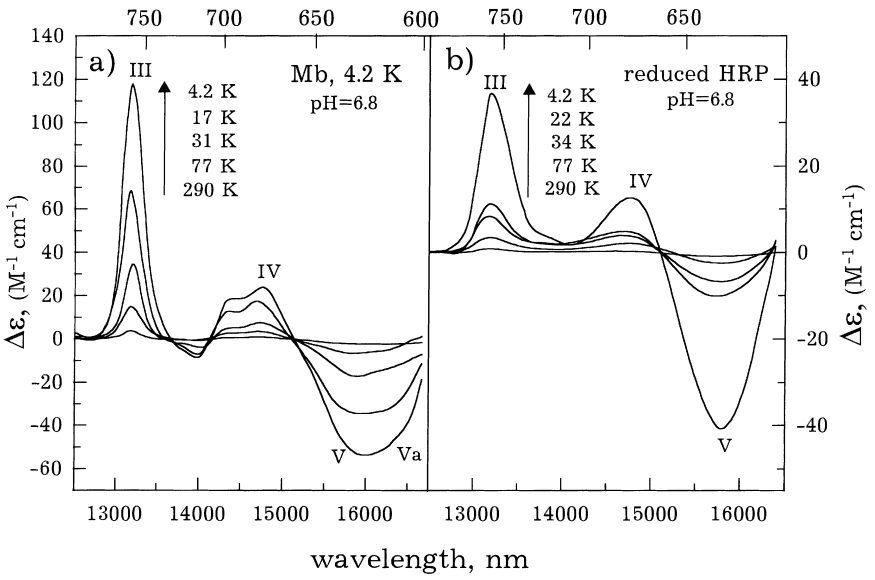

Fig. 1a, b. Temperature-dependent magnetic circular dichroism (MCD) spectra in the near-infrared region, recorded in a magnetic field of 1.45 T [28] for: **a** deoxy-myoglobin (Mb); **b** reduced horse radish peroxidase (HRP)

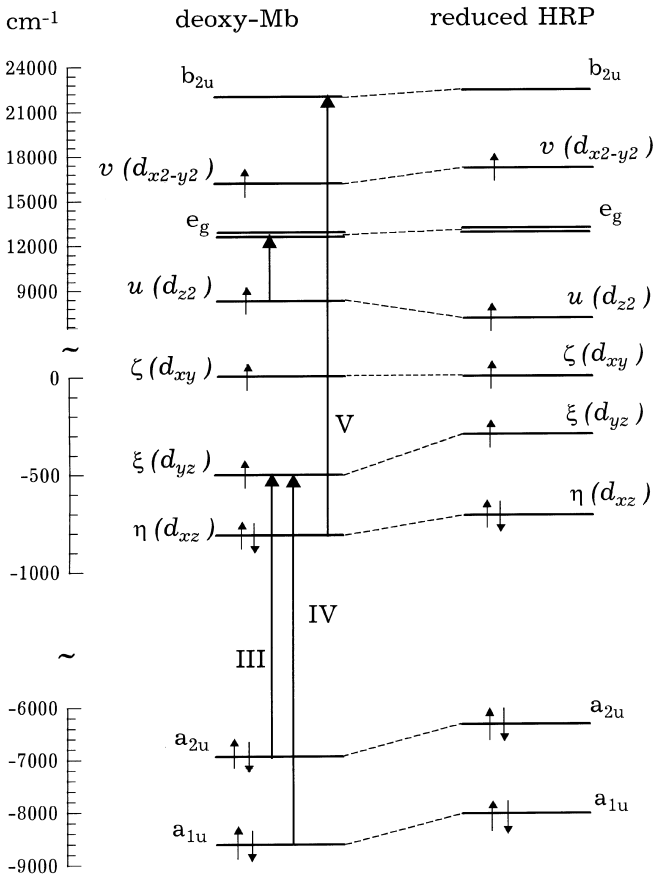

Fig. 2. One-electron level schemes for deoxy-Mb and reduced HRP, and the electron promotions responsible for the assigned transitions. Relative energies of molecular orbitals η, ξ, ζ, v and u mainly composed of the iron d-orbitals (shown in parentheses) are taken from [25]. Relative energies of porphyrin orbitals are estimated from energies of assigned transitions after taking into account exchange corrections. All energies are given relative to that of $\xi(d_{xy})$-orbital. The *arrows* show assigned one-electron transitions

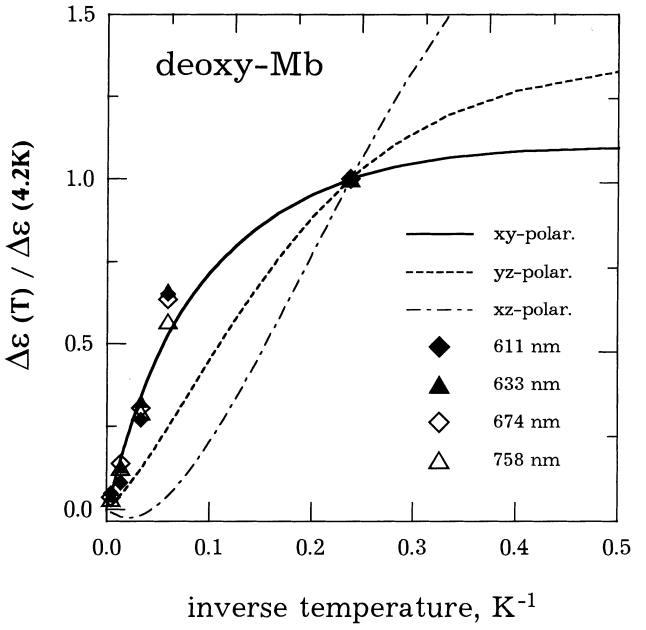

Fig. 3. Comparison of observed (*points*) and predicted (*lines*) temperature profiles of MCD intensity in the near-infrared region of deoxy-Mb at a magnetic field value of 1.45 T. The MCD intensity is normalized to that at 4.2 kelvin (K). The predicted profiles are calculated as ratios $g_i(T)/g_i$ (4.2 K), $i = x, y, z$

We exclude from the consideration the CT transitions involving promotion of an electron from the lower filled porphyrin orbitals, since our estimation shows that the energy of these transitions is outside the near-infrared region. As follows from columns six, seven and eight of Table 1 and analysis given for transitions to degenerate orbitals, only 11 transitions are allowed in MCD. Of these, the transitions $\overline{a}_{2u}(\pi), \overline{a}_{1u}(\pi) \rightarrow \overline{\xi}$; $\overline{\eta} \rightarrow \overline{b}_{2u}(\pi^*)$, $\overline{u}, \overline{v}; \zeta, u, v \rightarrow e_g(\pi^*)$ are either $x(y)$-, $y(x)$- or xy-polarized, the transition $\overline{\eta} \rightarrow \overline{e}_{gx}(\pi^*)$ is $z(y)$-polarized and two transitions, namely, $\overline{\eta} \rightarrow \overline{\zeta}$ and $\overline{\eta} \rightarrow \overline{b}_{1u}(\pi^*)$, have $y(x,z)$ polarization.

As shown in the previous section, the polarization of transitions is associated with the $g_i(T,H)$ factors which can be calculated using the ligand field parameters available [25]. Moreover, if transition is polarized in one plane, temperature dependence of MCD intensity normalized to an intensity at any temperature, is determined only by a corresponding $g_i(T,H)$ factor (Eq. 3). For a $y(x,z)$-polarized transition the normalized temperature dependence becomes a superposition of the $g_z(T,H)$ and $g_x(T,H)$ factors. Figures 3 and 4 compare observed and predicted temperature profiles of MCD intensity in the near-infrared region of Mb and HRP, respectively. The MCD intensity is normalized to that at 4.2 K. The predicted profiles are calculated as ratios $g_i(T)/g_i$ (4.2 K), i $= x, y, z$. In all spectral regions the experimental temperature dependences for both proteins coincide with the predicted ones for $x(y)$-, $y(x)$- or xy- polarization.

We start with the assignments of bands III (760 nm) and IV (675 nm). These bands polarized in the xy plane are positive in MCD and, therefore, the transitions $\overline{a}_{2u}(\pi), \overline{a}_{1u}(\pi) \rightarrow \overline{\xi}, \overline{\eta} \rightarrow \overline{u}$ and $\zeta, u, v \rightarrow e_g(\pi^*)$ can be considered as candidates. According to the single-crystal polarization data of Eaton et al. [2] on deoxy-Hb both bands are polarized in the porphyrin plane but in different directions, mainly in the x and y ones, respectively. Transitions of the $a_1, a_2, b_1, b_2 \rightarrow e$ type should have xy polarization. In addition, bands III and IV are simple not composite, while a superposition of four bands is expected for promotion of an electron to a degenerate $e_g(\pi^*)$ orbital. Hence, we ruled out $\zeta, u, v \rightarrow e_g(\pi^*)$ promotions from our consideration. The transition $\overline{\eta} \rightarrow \overline{u}$ can also be excluded, since calculation of the relative energies of d-orbitals (Fig. 2) put the transition $\overline{\eta} \rightarrow \overline{u}$ at $\sim$9100 cm^{-1}(1100 nm) and at $\sim$7800 cm^{-1}(1300 nm) for Mb and HRP, respectively. Thus, the transitions $\overline{a}_{2u}(\pi), \overline{a}_{1u}(\pi) \rightarrow \overline{\xi}$ from the nearly degenerate orbitals a_{2u} and a_{1u}, with a_{2u} lying above a_{1u}, are most likely responsible for bands III and IV, respectively. Our assignments are consistent with the tentative assignments of bands III and IV in deoxy-Hb given by Eaton et al. [2].

Since we now know the energies of $\overline{a}_{2u}(\pi), \overline{a}_{1u}(\pi) \rightarrow \overline{\xi}$ transitions, we are able to evaluate the excitation energies for all $d \rightarrow e_g(\pi^*)$ promotions:

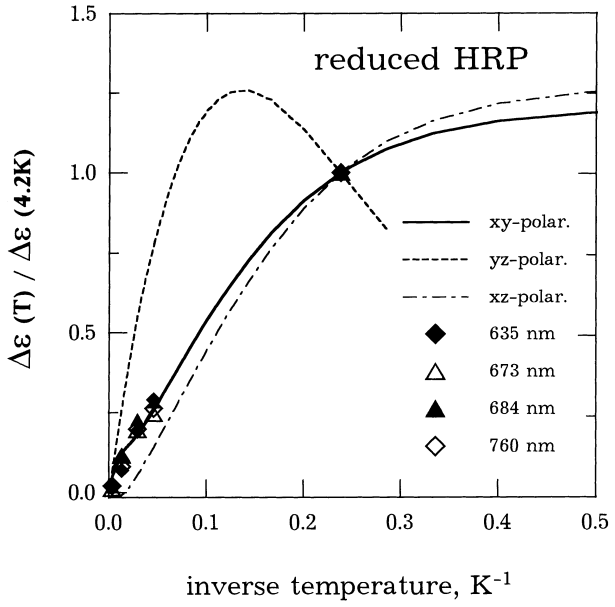

Fig. 4. Comparison of observed (*points*) and predicted (*lines*) temperature profiles of MCD intensity in the near-infrared region of reduced HRP at a magnetic field value of 1.45 T. The MCD intensity is normalized to that at 4.2 K. The predicted profiles are calculated as ratios $g_i(T)(4.2\text{ K}),\ i = x, y, z$

$$W(d \to e_g(\pi^*)) \approx \frac{W_S(\pi \to \pi^*) + W_V(\pi \to \pi^*)}{2} - \frac{W(\overline{a}_{2u} \to \overline{\xi}) + W(\overline{a}_{1u} \to \overline{\xi})}{2} + \alpha^2 \cdot \Delta + w(\xi) - w(d)\ , \qquad (5)$$

where $W_S(\pi \to \pi^*)$ and $W_V(\pi \to \pi^*)$ are the observed average energies of the $\pi - \pi^*$ transitions in the Soret and visible regions, respectively; Δ is an exchange energy correction calculated from exchange corrections to orbital energy differences [2] and is estimated to be $\sim$19000 cm^{-1} and $\sim$20100 cm^{-1} for $d = \zeta, v$ and $d = u$, respectively; α^2 is a covalency constant evaluated to be 0.71 and 0.75 for Mb and HRP, respectively [25], and $w(\xi) - w(d)$ is a d-orbital energy difference shown in Fig. 2.

Substituting appropriate values for Mb and HRP into the above expression gives, respectively:

$$W(u \to e_g) \approx 11879\text{ cm}^{-1}, W(v \to e_g) \approx 3286\text{ cm}^{-1}, W(\xi \to e_g) \approx 19385\text{ cm}^{-1};$$
$$W(u \to e_g) \approx 13952\text{ cm}^{-1}, W(v \to e_g) \approx 3001\text{ cm}^{-1}, w(\zeta \to e_g) \approx 20207\text{ cm}^{-1}\ .$$

Of these transitions, only $u \to e_g(\pi^*)$ falls in the near-infrared region. As pointed out in the previous section, the promotion of an electron from a nongenerate orbital to the degenerate porphyrin $e_g(\pi^*)$ orbital gives rise to superposition of four *xy*-polarized MCD bands. Therefore, we assign to this transition overlapping *xy*-polarized bands, observed between bands III and IV in the MCD spectra of both Mb and HRP (Fig. 1a, b).

We turn now to negative MCD observed in the 15200–16500 cm^{-1} (600–650 nm) region. There is a superposition of at least two bands in the MCD spectra of Mb while the presence of the second band is not apparent in the spectra of HRP (Fig. 1a and b, respectively). Table 1 shows that negative MCD bands can originate form either $\overline{\eta} \to \overline{v}(d-d)$ or $\overline{\eta} \to \overline{b}_{2u}(\pi^*)$ CT transition. The $\overline{\eta} \to \overline{v}$ transition is predicted to lie in the visible region at 16910 cm^{-1} (591 nm) for Mb and 17920 cm^{-1} (558 nm) for HRP (Fig. 2). Therefore, we assign band V, seen in the MCD spectra of both proteins at $\sim$15800 cm^{-1} (634 nm), to the $\overline{\eta} \to \overline{b}_{2u}(\pi^*)$ CT transition. This assignment coincides with the prediction made by Seno et al. [20]. The origin of band Va, located at $\sim$16400 cm^{-1} (610 nm) in the MCD spectra of Mb, remains undetermined. One-electron promotions for the assigned transitions are shown by arrows in Fig. 2.

In order to visualize the individual contributions of the assigned transitions to the overall MCD spectra recorded at 4.2 K we carried out decomposition of observed spectra into Gaussian components arising from a given transition. Figures 5 and 6 display the results obtained for Mb and HRP, respectively. In a fit procedure for Mb we added the second-unassigned band in the high-energy region. The MCD arising from the $u \to e_g(\pi^*)$ transition consist of four bands and is shown by a dashed line (Fig. 5).

Now we will attempt to correlate behaviour of the assigned transitions with local haem structure changes and compare predictions with available observations. X-ray structure data show that an imidazole plane in deoxy-Mb [30] and deoxy-Hb [31] as well as in five-coordinate haem model complexes [32] approximately eclipses Fe-N(porphyrine) bonds rather than making an angle of 45° with them. Extensive calculations [32] point at the Fe-N(imidazole) π bond as the stabilizing factor for such an orientational preference. As a result, the $\xi(d_{yz})$-orbital acquires an antibonding character and becomes higher in energy. The $\eta(d_{xz})$-orbital contributes much less to the Fe(π)-imidazole(π) interaction than the $\xi(d_{yz})$-orbital, and its energy has to be relatively insensitive to this interaction. A rhombicity at the haem results in the difference between the antibonding characters of the two orbitals. From this, one can predict that the red shift of bands III and IV, associated with the $\overline{a}_{2u}(\pi), \overline{a}_{1u}(\pi) \to \overline{\xi}$ transitions, respectively, and approximately invariability of an energy of band V assigned to the $\overline{\eta} \to \overline{b}_{2u}(\pi^*)$ CT transition, are the cause of a weakening of the Fe-N(imidazole) π bond.

Numerous studies of metastable photoproducts of CO complexes of haemoproteins, either generated at 4.2 K [1, 6, 8–10] or observed using the time-resolved technique [11–18], are in line with these predictions. MCD spectra, in which all three bands are well resolved, are more informative in comparison with absorption ones where only band III is resolved. Figures 4 and 5 compare the near-infrared MCD spectra of photoproducts, generated by illumination at 4.2 K of CO complexes of Mb and neutral HRP, respectively, with those of room temperature preparations of five-coordinate adducts.

After photodissociation of a ligand at cryogenic temperatures, the geometry of Fe-porphyrin and Fe-His

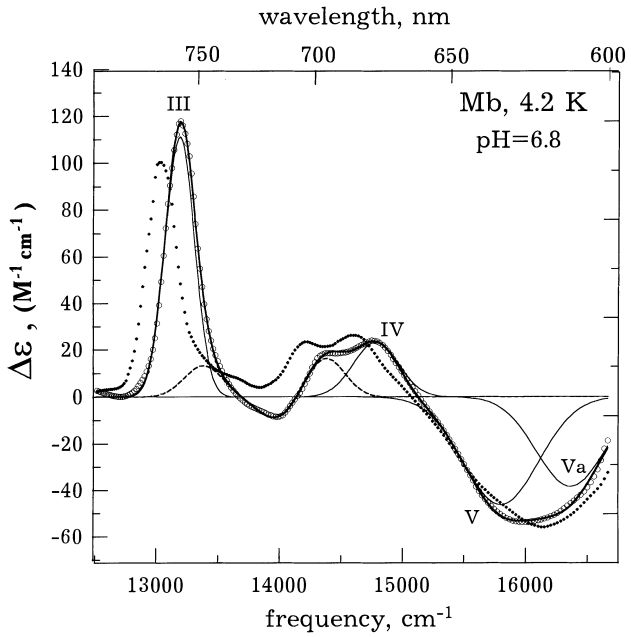

Fig. 5. Decomposition of the near-infrared MCD spectrum of deoxy-Mb into components and a comparison between the MCD spectrum of the deoxy-preparation (*open circles*) and that of the photoproduct of its CO complex generated at 4.2 K (*filled circles*). The MCD spectrum of deoxy-Mb is decomposed into eight Gaussian components. The *thin solid lines* show the components approximating bands III, IV, V and the unassigned high-energy band. The *dotted line* shows the sum of four components arising from a $u(d_{z2}) \rightarrow e_g(\pi^*)$ CT transition. The *thick solid line* is the sum of all Gaussian components. The data is taken from [9]

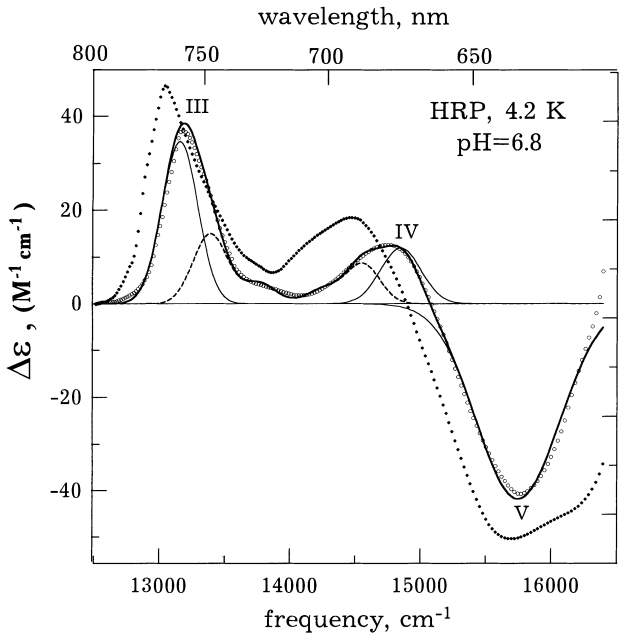

Fig. 6. Decomposition of the near-infrared MCD spectrum of reduced HRP into its components and a comparison of the MCD spectrum of the reduced enzyme (*open circles*) with that of the photoproduct of its CO complex generated at 4.2 K (*filled circles*). The MCD spectrum of reduced HRP is decomposed into seven Gaussian components. The *thin solid lines* show the components approximating bands III, IV and V. The *Dotted line* shows the sum of four components arising from a $u(d_{z2}) \rightarrow e_g(\pi^*)$ CT transition. The *thick solid line* is the sum of all Gaussian components. The data is taken from [8]

bonds remains mainly the same as in the ligated haem before photolysis [9, 25]. It is well known [33] that in a five-coordinate haem the iron is displaced out of a porphyrin plane and moves to the plane in a six-coordinate haem. This movement has to be accompanied by a weakening of the Fe-His bond. The red shift of bands III and IV in an unrelaxed metastable photoproduct as compared to a relaxed equilibrium five-coordinate haem, displayed in Figs. 5 and 6, is consistent with our assignment of these bands. Similar results have been obtained for Hb and a protein-free protohaem-(2-methylimidazole) complex [9, 25]. The value of the shift depends on the protein origin and the type of ligand photodissociated. The findings were interpreted as the difference in restrictions imposed by different protein moieties on the local haem structure upon ligand binding. It is also important to note that, as expected, band V in the MCD spectra of the metastable photoproducts remains essentially unshifted relative to its position in the relaxed haem state.

The 15-nm red shift of band III in the absorption spectra observed by Sage et al. [15] on a breakage of the Fe-His bond in deoxy-Mb at low pH is further confirmation of the validity of our assignment for this band. The value of the shift is larger than that observed in photolysis experiments. This is consistent with our prediction, since in the four-coordinate haem the $\xi(d_{yz})$ orbital has to have a lower energy than in any five-coordinate haem.

Recently, Einarsdottir et al. [34] observed a band near 785 nm in the absorption spectra of fully reduced unligated cytochrome *c* oxidase and a photoproduct of its CO complex. The authors attributed this band to the unligated ferrous haem a_3 and considered it as an analogue of band III in deoxy-Mb and deoxy-Hb. The haem a_3 in cytochrome *c* oxidase apparently has a unique structure and differs from the protohaem found in other haemoproteins by replacement of one of four methyl groups by the long alkyl chain [35]. According to our assignment of band III, we explain the $\sim$25-nm red shift to this band in cytochrome *c* oxidase, as compared to its position in other high-spin ferrous haemoproteins discussed above, by an increase of energy of the $a_{2u}(\pi)$-porphyrin orbital due to withdrawal of π-electron density from the porphyrin to the alkyl substituent.

Besides the above bands, two other positive MCD bands have been observed by Eaton et al. [2] in the room temperature MCD spectrum of deoxy-Hb. Bands I and II are located at 11000 cm^{-1} and 12400 cm^{-1}, respectively. The authors assigned band I to $\overline{\eta} \rightarrow \overline{e}_g(\pi^*)$ transition and suggested two promotions, namely, $\overline{\eta} \rightarrow \overline{u}$ and $\overline{a}_{2u} \rightarrow \overline{\zeta}$ as possible assignments of band II. According to Table I, the $\overline{a}_{2u} \rightarrow \overline{\zeta}$ transition is ineffective in MCD and therefore must be ruled out from the consideration. The signs of the MCD bands for two other ones are predicted to be positive and therefore do not contradict the assignment given by Eaton et al. [2].

Up to now we have discussed the near-infrared bands in spectra of high-spin ferrous haemoproteins where the protein-derived ligand is an imidazole of a histidine. Attempts to observe the near-infrared bands in MCD spectra of reduced cytochrome P450, at protein concentrations used in the studies of other haemoproteins, appeared to be unsuccessful [36]. Cytochrome P450 has a sulphur anion of cysteine as a proximal haem iron ligand and the ground electronic state in the reduced enzyme is $^5B_2$ rather than $^5E_\eta$ as seen in other proteins [25].

The change of the ground electronic state in reduced cytochrome P450 has two consequences. All the bands considered above are shifted in energy. Secondly, as shown in the previous section, the intensities of these bands in MCD and absorption have to be decreased at least by a factor of 0.1 and 0.01, respectively as compared to the intensity in haemoproteins containing histidine as the protein-derived ligand of the haem iron. MCD and absorption, which are the first-and zero-order effects, respectively, in Mb and HRP, become the second-order effects in cytochrome P450. Therefore, very high enzyme concentration are required to detect these bands in MCD or absorption spectra of cytochrome P450. Indeed, Nozava et al. [37] could observe very weak MCD bands in the near-infrared region of reduced cytochrome P450 using a 5-mm cell at enzyme concentrations up to 1.3 mM.

Acknowledgements: We thank RFFI (grant 96-04-49076) and ISF (grant N25300) for financial support.

References

1. Iizuka T, Yamamoto H, Kotani M, Yonetani T (1974) Biochim Biophys Acta 371:126–139
2. Eaton WA, Hanson LK, Stephens PJ, Sutherland JC, Dunn JBR (1978) J Am Chem Soc 100:4991–5003
3. Cordone L, Cupane A, Leone M, Vittrano E (1986) Biophys Chem 24:259–275
4. Chaves MD, Courtney SH, Chance MR, Kiula D, Nocek J, Hoffman BM, Fridman M, Ondrias MR (1990) Biochemistry 28:4844–4852
5. Nozawa T, Yamamoto T, Hatano M (1976) Biochim Biophys Acta 427:28–37
6. Sharonov YuA, Sharonova NA, Figlovsky VA, Grigorjev VA (1982) Biochim Biophys Acta 709:332–341
7. Sharonov YuA, Figlovsky VA, Sharonova NA, Mineyev AP (1983) Biophys Struct Mech 10:47–59
8. Sharonov YuA, Pysmensky VF, Yarmola EG (1988) FEBS Lett 235:63–66
9. Sharonov YuA, Pismensky VF, Yarmola EG (1989) J Biomol Struct Dyn 7:207–224
10. Fiamingo FG, Alben JO (1985) Biochemistry 24:7964–7970
11. Ansari A, Berendzen J, Bowne SF, Frauenfelder H, Iben IET, Sauke TB, Shyamsunder E, Young RD (1985) Proc Natl Acad Sci USA 82:5000–5004
12. Campbell BF, Chanse MR, Friedman JM (1987) Science 238:373
13. Agmon N (1988) Biochemistry 27:3507–3511
14. Steinbuch PJ, Ansari A, Berendzen J, Braunstein D, Chu K, Cowen BR, Ehrenstein D, Frauenfelder H, Johnson JB, Lamb DC, Luck S, Mourant JR, Nienhaus GU, Ormos P, Philipp R, Scholl R, Xie A, Young RD (1991) Biochemistry 30:3988–4001
15. Srajer V, Champion PM (1991) Biochemistry 30:7390–7402
16. Nienhaus GU, Mourant JR, Frauenfelder H (1992) Proc Natl Acad Sci USA 89:2902–2906
17. Nienhaus GU, Mourant JR, Chu K, Frauenfelder H (1994) Biochemistry 33:13413–30
18. Sassaroli M, Rousseau DL (1987) Biochemistry 26:3092–3098
19. Seno Y, Kameda N, Otsuka J (1980) J Chem Phys 72:6048–6058
20. Seno Y, Kameda N, Otsuka J (1980) J Chem Phys 72:6059–6069
21. Makinen MW, Churg AK (1983) In: Lever ABP, Gray HB (eds) iron porphyrins. Addison-Wesley, Reading, Mass, pp 141–235
22. Sage GT, Morikis D, Champion PM (1991) Biochemistry 30:1227–1237
23. Collman JP, Hoard JL, Kim N, Lang G, Reed CA (1976) J Am Chem Soc 97:2676–2681
24. Lang G, Spartalian K, Reed CA, Collman JP (1978) J Chem Phys 69:5424–5427
25. Oganesyan VS, Sharonov YuA (1997) Spectrochim Acta 53 A:433–449
26. Eicher H, Trautwein A (1969) J Chem Phys 50:2540–2551
27. Schatz PN, Mowery RL, Krausz ER (1978) Mol Phys 35:1537–1557
28. Sharonov YuA (1991) In:Skulachev VP (ed.) Sov Sci Rev D (Physicochemical biology vol 10, part 3) Harwood, London, pp 1–118
29. Zerner M, Gouterman M, Kobayashi H (1966) Theor Chim Acta 6:363–400
30. Takano T (1977) J Mol Biol 110:569–584
31. Fermi G, Perutz MF, Shaanen B, Fourme R (1984) J Mol Biol 175:159–174
32. Scheidt WR, Chipman DM (1986) J Am Chem Soc 108:1163–1167
33. Perutz MF, Fermi G, Luisi B, Shaanan B, Liddington RC (1987) Acc Chem Res 20:309–321
34. Einarsdottir O, Georgiadis KE, Dawes TD (1992) Biochim Biophys Res Commun 184:1035–1041
35. Caughey WS, Smythe GA, O'Keeffe DH, Maskasky J, Smyth ML (1975) J Biol Chem 250:7602–7622
36. Sharonov YuA, Pismensky VF, Greschner S, Ruckpaul K (1987) Biochim Biophys Res Commun 146:165–172
37. Nozawa T, Shimizu T, Hatano T, Shimada H, Iizuka T, Ishimura Y (1978) Biochim Biophys Acta 534:285–294